Acta Crystallographica Section D
Biological Crystallography
ISSN 0907-4449

The structure of a mutant enzyme of *Coprinus cinereus* peroxidase provides an understanding of its increased thermostability

Karen Houborg,[a] Pernille Harris,[a] Jens-Christian Navarro Poulsen,[a] Palle Schneider,[b] Allan Svendsen[b] and Sine Larsen[a]*

[a]Centre for Crystallographic Studies, University of Copenhagen, Universitetsparken 5, 2100 Copenhagen, Denmark, and [b]Novozymes A/S, Smørmosevej 25, 2880 Bagsvaerd, Denmark

Correspondence e-mail: sine@ccs.ki.ku.dk

Received 27 October 2002
Accepted 24 March 2003

PDB Reference: thermostable mutant CiP, 1ly8, r1ly8sf.

Seven amino-acid substitutions introduced into the 343 amino-acid-long sequence of *Coprinus cinereus* peroxidase (CiP) led to a mutant enzyme (TS-rCiP) which is more stable than the native enzyme at higher temperature, pH and hydrogen peroxide concentrations. It is therefore more suitable for industrial applications. A structure determination was conducted on a deglycosylated but still active form of TS-rCiP based on X-ray diffraction data to 2.05 Å resolution measured on a crystal cooled to 100 K and refined to R = 0.202 and $R_{\rm free}$ = 0.249. The increased stability of the TS-rCiP enzyme can be understood from the structural changes of the TS-rCiP structure revealed by a comparative analysis with other known CiP structures. One of the more significant changes caused by three of the substitutions, I49S, V53A and T121A, is the conversion of a hydrophobic pocket into a hydrophilic pocket with associated changes in the water structure and the hydrogen-bonding interactions. The E239G substitution, which gives rise to increased thermostability at high pH, creates changes in the water structure and in the orientation of a phenylalanine (Phe236) in its vicinity. The three substitutions M166F, M242 and Y242F introduced to increase the oxidative stability do not introduce any structural changes.

1. Introduction

The haem-containing peroxidases (EC 1.11.1.7) convert a two-electron oxidation process into two one-electron processes in a catalytic cycle involving two oxidized intermediates which react directly with the substrate. The ability of peroxidases to oxidize a broad spectrum of small organic molecules makes them interesting from an industrial point of view. One of the peroxidases with a significant commerical potential is from the ink cap *Coprinus cinereus* (CiP). Among its applications is its function as a catalyst in the oxidation of dyes which leach out of coloured clothes during the wash cycle. It decolourizes the dye and prevents dye transfer to other clothes (Cherry *et al.*, 1999). The use of native CiP as an enzyme in the bleaching process is limited by its decreased stability at high pH (10.5), high temperatures (323 K) and high peroxide concentrations (5–10 m*M*) (Cherry *et al.*, 1999). This initiated a search for mutant enzymes which would function better under these harsh conditions (Cherry *et al.*, 1999).

CiP belongs to class II of the superfamily of plant peroxidases, which comprises a variety of peroxidases and ligninases (Welinder, 1992). Native CiP consists of a 38 kDa single polypeptide chain composed of 343 amino acids and a haem group. It is anionic, with a pI of 3.5 (Kjalke *et al.*, 1992). The structure at 274 K of the native glycosylated recombinant CiP (rCiP; PDB code 1h3j) has been determined (Petersen *et*

al., 1994). CiP has been shown to be almost identical to the peroxidase from *C. macrorhizus* and *Arthromyces ramosus* (ARP). The former differs from CiP in its glycosylation pattern (Kjalke *et al.*, 1992), while the latter enzyme differs not only in its glycosylation but also has one additional glycine in the N-terminus (Kjalke *et al.*, 1992; Sawai-Hatanaka *et al.*, 1995). Since the glycosylated rCiP turned out to be very difficult to crystallize (Petersen *et al.*, 1993), a mutant enzyme was constructed in which all the potential N- and O-glycosylation (A142S, T331A and S338A) sites were removed. This mutant enzyme rCiPON proved to be easier to crystallize and an investigation of this enzyme at room and cryogenic temperature (rCiPON-RT and rCiPON-LT; PDB codes 1ly9 and 1lyc, respectively) has recently been carried out (Houborg *et al.*, 2003).

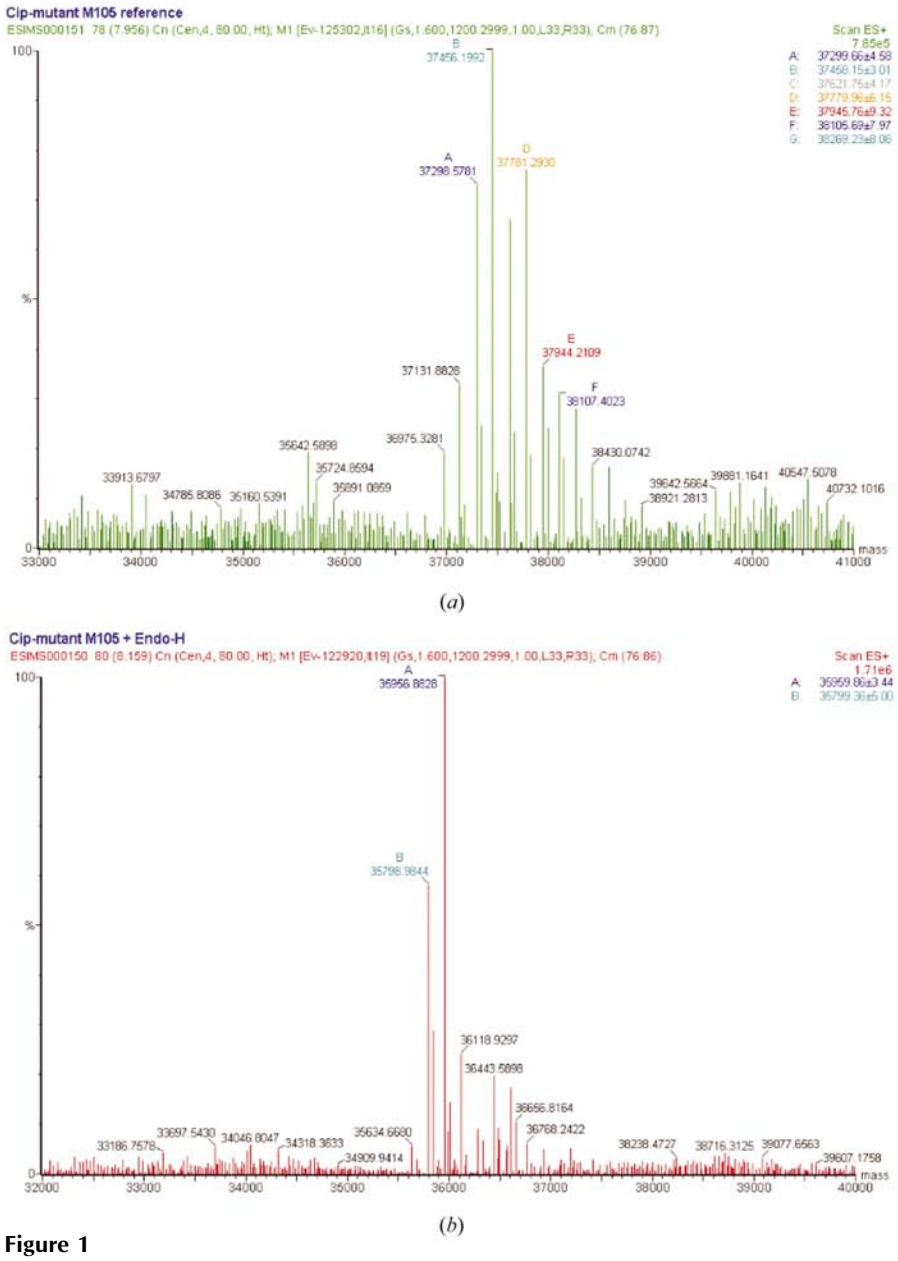

Figure 1
Mass spectra of TS-rCiP: (*a*) before deglycosylation, (*b*) after deglycosylation.

The search for a mutant enzyme of CiP which would be more suitable for industrial purposes resulted in a recombinant CiP with intact glycosylation sites (Asn142, Thr331 and Ser338) and seven amino-acid substitutions (TS-rCiP; Cherry *et al.*, 1999). Three of the seven amino-acid substitutions were selected to increase the oxidative stability (M166F, M242I, Y272F), as methionines and tyrosines are known to be oxidized by hydrogen peroxide (Cherry *et al.*, 1999). Another was designed to improve the thermostability at high pH (E239G; Cherry *et al.*, 1999). The last three substitutions (I49S, V53A, T121A) increased, either independently or synergistically, both the thermostability and the oxidative stability (Cherry *et al.*, 1999). The pI of TS-rCiP is 3.5 (data not shown), which is identical to the pI of the native enzyme. TS-rCiP and native CiP have approximately the same specific activity at pH 7 (Cherry *et al.*, 1999). At pH 10.5, TS-rCiP shows only 0.05 times the activity of native CiP; however, it is 100 times more stable towards hydrogen peroxide than native CiP (Cherry *et al.*, 1999). The thermostability of TS-rCiP was calculated as 174 times the stability of native CiP, where thermostability was determined as the activity remaining after 5 min incubation of the enzyme at 313 K and pH 10.5 (Cherry *et al.*, 1999).

The structure determination of TS-rCiP presented here provides the structural background for its increased stability.

2. Materials and methods

2.1. Deglycosylation of the enzyme

TS-rCiP was expressed and purified as described previously (Cherry *et al.*, 1999). TS-rCiP was treated with the deglycosylation enzyme recombinant endoglycosidase H (Endo-H; EC 3.2.1.96) purchased from Roche (Cat. No. 1088726). TS-rCiP was deglycosylated at 277 K for 3 d under the following experimental conditions: 21 mg mutant enzyme, 2.1 U Endo-H and 10.7 ml acetate buffer pH 5.5.

Mass spectrometry was used to validate the treatment with Endo-H. The mass spectrometer used was a VG-Platform from Micromass coupled to a Waters HPLC system with electrospray ionization. The mass spectrum, which was recorded prior to deglycosylation, shows that TS-rCiP was heterogeneously glycosylated and that the protein sample contains different glycosylated species with masses varing between 37 and

39 kDa (Fig. 1). The mass spectrum of TS-rCiP after the treatment with Endo-H is also depicted in Fig. 1. The protein mass varies after deglycosylation between 35.7 and 36.7 kDa, with a major peak at 35 957 Da. After the treatment with Endo-H, TS-rCiP was dialysed against water and then concentrated. Measurements with a HP 8452A diode-array spectrometer were used to estimate the purity of the protein sample. The final R_z (OD_{404}/OD_{280}) was 3.3 for TS-rCiP.

2.2. Crystallization

Crystals of TS-rCiP were obtained by the vapour-diffusion method using hanging drops. A protein solution with a concentration corresponding to an OD_{280} of 8.6 and an OD_{404} of 27 was used for the experiments. The suitability of the protein concentration was checked by performing a footprint screen (Stura *et al.*, 1992) at 293 K. The subsequent crystallization experiments carried out at 293 K using Crystal Screens I and II (Cudney *et al.*, 1994) resulted in drops with phase separation, precipitate and spherulites. Optimizations were made around the conditions (1.5 *M* ammonium sulfate and 0.1 *M* sodium acetate pH 5.5) in which spherulites were observed. Stacked plates appeared against a reservoir solution composed of 0.1 *M* 2-(*N*-morpholino)ethanesulfonic acid (MES) pH 6.2 and 1.6 *M* ammonium sulfate at 277 K in drops made of 2 µl TS-rCiP plus 2 µl reservoir solution.

Single crystals could be obtained as thin plates by microseeding, which was conducted as follows. A stack of the largest plates were removed from the drop and washed in the reservoir solution before being crushed in a seed bead (Cudney *et al.*, 1994) with 15 µl of the reservoir solution. From the stock solution, two dilutions (×10, ×100) were made. A horse hair was used to seed from the stock solution and the two dilutions into drops, which were pre-equilibrated for 2 d in the metastable zone (1.6 *M* ammonium sulfate and 0.1 *M* MES pH 6.2). The best results were achieved with seeds from the stock solution. This gave drops which contained thin single crystals in addition to stacks of plates. Crystals of TS-rCiP obtained this way similar to that which diffracted to 2.05 Å are shown in Fig. 2.

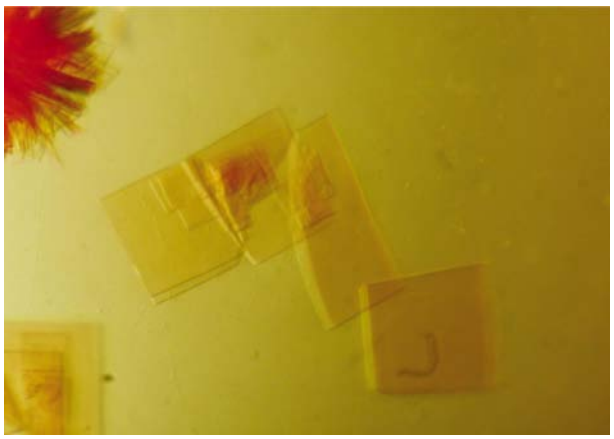

Figure 2
Crystals of TS-rCiP similar to that which diffracted to 2.05 Å. The length of the plates is approximately 0.12 mm.

Table 1
Data-collection and refinement statistics.

Values in parentheses are for the outermost resolution shell.

Space group	$P2_12_12$
Unit-cell parameters (Å)	a = 74.49, b = 114.86, c = 73.61
Resolution (Å)	20.0–2.05 (2.10–2.05)
Completeness (%)	91.6 (89.4)
Total No. of reflections	110655
No. of unique reflections	35855
Mosaicity (°)	0.27–0.66
R_{merge}†	0.086 (0.186)
Redundancy	3.1
No. of haem groups	2
No. of calciums	4
No. of waters	637
No. of glycerols	12
No. of carbohydrates	6
R/R_{free}	0.202/0.249
R.m.s. deviation	
Bonds (Å)	0.014
Angles (°)	1.4

† $R_{merge} = \sum_{hkl}\sum_i |I_{hkl} - \langle I_{hkl}\rangle|/\sum_{hkl}\sum_i \langle I_{hkl}\rangle$.

2.3. Data collection and processing

Data were collected at MAX-lab, Lund on beamline I711 (Cerenius *et al.*, 2000) at cryogenic temperature (T = 100 K). For cryoprotection, the crystal was transferred to a solution where 27% glycerol was added to the reservoir solution. The crystals were very thin and the diffraction depended critically on their thickness. The best crystal diffracted to a maximum resolution of around 2.05 Å. The data were collected from this crystal. The resolution was set to avoid ice rings which appeared owing to fluctuation in the cryostream.

The data were merged and integrated using the *HKL* program suite (Otwinowski & Minor, 1997). The data-collection and processing statistics are given in Table 1. The variation in mosaicity is attributed to the shape of the crystal, which was a very thin plate. This is also the likely cause of the variation of the quality of the data with oscillation range. As the ice rings seriously affected the quality of the data within the limits 3.29–3.22, 2.82–2.78, 2.54–2.49 and 2.31–2.27 Å, it was decided to remove the reflections in these regions from the data set, even though this resulted in a decreased completeness (see below).

2.4. Structure solution and refinement

The structure was solved by molecular replacement using the program *AMoRe* (Navaza & Saludjian, 1997). The 1.57 Å structure of rCiPON-LT (PDB code 1lyc) without the calcium ions was used as a search model. A solution with a correlation factor of 62.9% and an R factor of 42.7% was found in space group $P2_12_12$. This was in agreement with the Laue symmetry and the systematically absent reflections $h00$ where $h = 2n + 1$ and $0k0$ where $k = 2n + 1$. The asymmetric unit contains two monomers (A and B). They are related to each other by the translation vector (0.081, 0.501, 0.509).

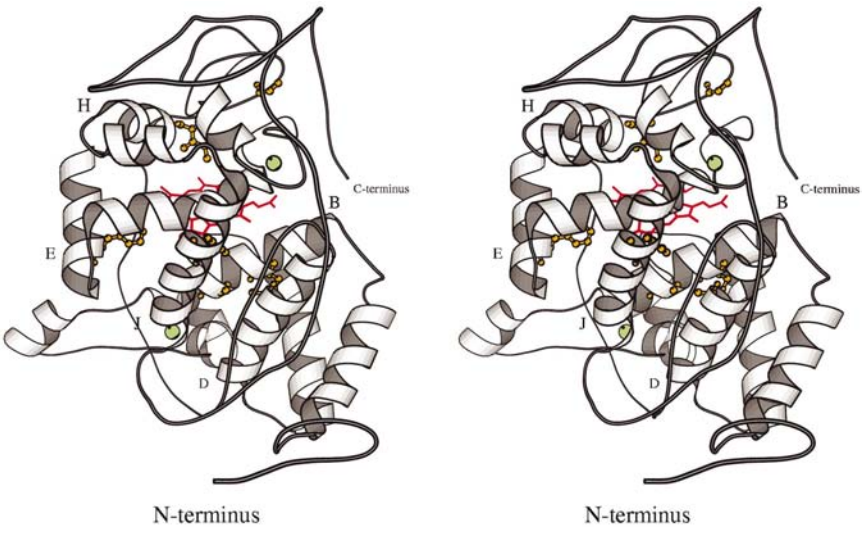

Figure 3
A schematic representation of TS-rCiP showing the fold and the substituted sites. The haem group is in red, the two calcium ions are in green and the seven substitution sites are in orange: I49S and V53A in helix *B*, T121A in helix *D*, M166F in helix *E*, E239G in a loop region, M242I close to helix *H* and Y272F in helix *J*. The figure is a stereoview prepared using the program *MOLSCRIPT* (Kraulis, 1991).

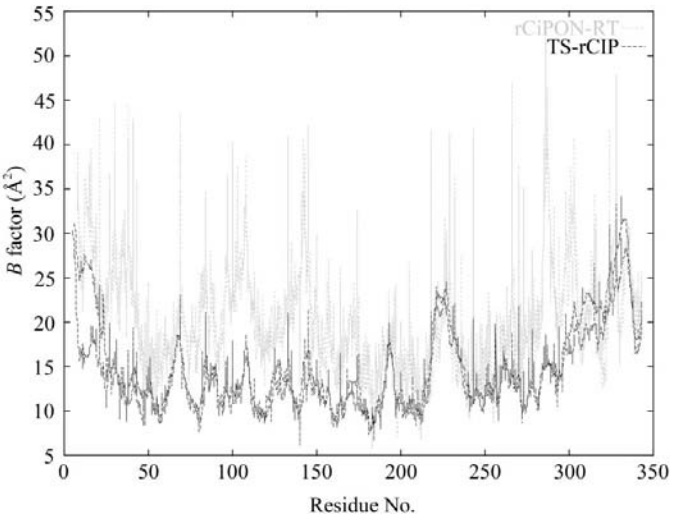

Figure 4
B factors as a function of residue number for the two molecules of TS-rCiP and rCiPON-RT.

The structure was refined using *CNS* v. 0.9 (Brünger *et al.*, 1998). An initial round of refinement was performed using non-crystallographic symmetry (NCS) restraints between the two molecules in the asymmetric unit. An examination of the electron-density map using the program *TURBO-FRODO* (Roussel & Cambillau, 1992) at the substituted sites showed a large discrepancy between the model and the electron-density map. All the exchanged residues were changed to the correct amino acids. The electron density clearly indicated the existence of the same calcium sites as in the other CiP structures. Four calcium ions were therefore included in the model. Additionally, the conformation of several other residues were modified. A subsequent refinement gave R and $R_{\rm free}$ factors of 0.302 and 0.347, respectively. The next rounds of refinements hardly changed the $R_{\rm free}$ factor. Several attempts to obtain a better model of the structure were conducted without any success. Since the R and $R_{\rm free}$ values were much higher in the resolution limits where ice rings occurred, all the reflections within these limits were removed. This gave R and $R_{\rm free}$ values of approximately 0.30 and 0.32, respectively. At this stage, water and glycerol molecules could be included in the structural model when good density was present in both the $2F_o - F_c$ and $F_o - F_c$ maps and was consistent with sensible hydrogen-binding geometry. Carbohydrate residues were included as there was evidence for them in both the $2F_o - F_c$ and the $F_o - F_c$ maps; they comprise an N-linked *N*-acetylglucosamine at residue Asn142 and two O-linked mannoses, one at residue Thr331 and the other at residue Ser338. From evidence in both $2F_o - F_c$ and $F_o - F_c$ maps, the following residues were refined in multiple configurations: Asp30*A*, Asn108*A*, Met279*A*, Ser280*A*, Leu281*A*, Asp30*B*, Asn108*B*, Ser131*B*, Met279*B* and Ser280*B*. The final round of refinement, where the k_b value in the parameter file for the haem group was set to 10, a bulk-solvent correction was performed and the NCS restraints were released, yielded $R = 0.202$ and $R_{\rm free} = 0.249$. The refinement statistics are given in Table 1. The program *PROCHECK* (Collaborative Computational Project, Number 4, 1994) was used to validate the quality of the final structure. 92% of the residues are in the most favoured regions and the remaining residues are in the additionally allowed regions.

3. Results and discussion

3.1. The structure of the mutant enzyme

Severe difficulties had previously been encountered in the crystallization of glycosylated rCiP (Petersen *et al.*, 1993). To overcome some of the difficulties associated with crystallizing a glycosylated protein, TS-rCiP was successfully deglycosylated with the deglycosylation enzyme Endo-H prior to crystallization. The activity of TS-rCiP measured after deglycosylation was found to be comparable to the activity of glycosylated TS-rCiP (data not shown). Data were collected to 2.05 Å resolution at cryogenic temperatures from one of the crystals. The structure was solved by molecular replacement in space group $P2_12_12$ and subsequently refined to $R = 0.202$ and $R_{\rm free} = 0.249$.

Like the other structures of CiP (Petersen *et al.*, 1994; Houborg *et al.*, 2003), the asymmetric unit contains two monomers. In TS-rCiP, they are almost related by the translation vector $(b/2) + (c/2)$. The two molecules comprise residues 5–343 (*A*) and 6–343 (*B*), each containing a haem

group, two structural calcium ions and carbohydrate moieties covalently attached to the three glycosylation sites. In addition, 12 glycerol and 637 water molecules are included in the model. The data were of sufficient quality to enable modelling of ten residues in multiple configurations. The first residues at the N-terminus are not visible in the electron-density map and are assumed to be disordered. The overall secondary structure (12 α-helices) of TS-rCiP (see Fig. 3) is identical to the secondary structure of CiP and ARP (Petersen *et al.*, 1994; Kunishima *et al.*, 1994; Houborg *et al.*, 2003).

3.2. Comparison of TS-rCiP with the CiP structures

The two independent molecules in TS-rCiP are identical; using the program *LSQMAN* (Kleywegt *et al.*, 2001), superposition of their C^{α} atoms gives an r.m.s. of 0.2 Å. This is similar to the results obtained for the other structures of CiP, which all contain two independent molecules. TS-rCiP will primarily be compared with the room-temperature structure rCiPON-RT and not with the other low-temperature structure rCiPON-LT, since the crystals used for data collection for rCiPON-LT were twinned. Twinned data have previously appeared to give unreliable thermal parameters and an unrealistically low number of water molecules (Harris *et al.*, 2002; Houborg *et al.*, 2003). The program *LSQMAN* (Kleywegt *et al.*, 2001) was used to superimpose the C^{α} atoms of TS-rCiP and rCiPON-RT, with a resultant r.m.s. of 0.57 Å. This indicates that the fold of TS-CiP is not significantly different from that of rCiPON-RT.

3.3. Temperature factors

Differences in *B* factors can reflect differences in temperature, packing environment and protein mobility, but may also depend on the refinement procedure. The value of the *B* factors plotted as a function of the residue numbers of the two molecules in the asymmetric unit of TS-rCiP and rCiPON-RT are shown in Fig. 4. As the data for TS-rCiP were collected at low temperature in contrast to rCiPON-RT, it is not unexpected that its *B* factors are generally lower and fluctuate less than those of rCiPON-RT. There are some differences in the *B* factors in the N-terminus of the *A* and *B* molecules in TS-rCiP which can be related to differences in crystal packing. Fig. 4 illustrates that the *B* factors are relatively lower for TS-rCiP in the regions formed by residues 25–45, 137–150 and 280–298. The substituted amino acids are not in any of these regions, which are confined to the surface of the protein. An analysis of the crystal contacts in TS-rCiP and rCiPON-RT using the program *CONTACTS* (Collaborative Computational Project, Number 4, 1994) suggests that the lower *B* factors in the regions consisting of residues 25–45 and residues 280–298 are a consequence of their involvement in crystal packing in TS-rCiP. However, crystal contacts cannot account for the lower *B* factors in the region

Table 2
Selected distances (Å) at the substituted amino acids I49S, V53A, T121A and E239G of TS-rCiP and rCIPON-RT.

	TS-rCiP	rCiPON-RT
I49S, V53A and T121A		
Ser49 O^{γ}—Ala121 N	3.16, 3.04	
W25—Ser49 O^{γ}	2.82, 2.84	
W25—Ser49 O	2.75, 2.79	
W25—Ile117 O	2.91, 2.97	
Ala53 O—Gln118 $N^{\varepsilon 2}$	3.38, 3.35	
Val53 $C^{\gamma 2}$—Gln118 $N^{\varepsilon 2}$		3.26, 3.32
Ile117 O—Thr121 O^{γ}		2.84, 2.81
E239G		
W38—W487	2.98, 2.78	
W487—Phe240 O	2.81, 2.76	
W1001—W1006		2.70, 2.87
W1006—Phe240 O		2.82, 2.63
W1001—Glu239 $O^{\varepsilon 1}$		2.95, 2.87
Glu214 $O^{\varepsilon 2}$—Glu239 $O^{\varepsilon 2}$		2.43, 2.58
Phe236 C^{β}—Pro237 C^{δ}	3.57, 3.58	3.13, 3.20

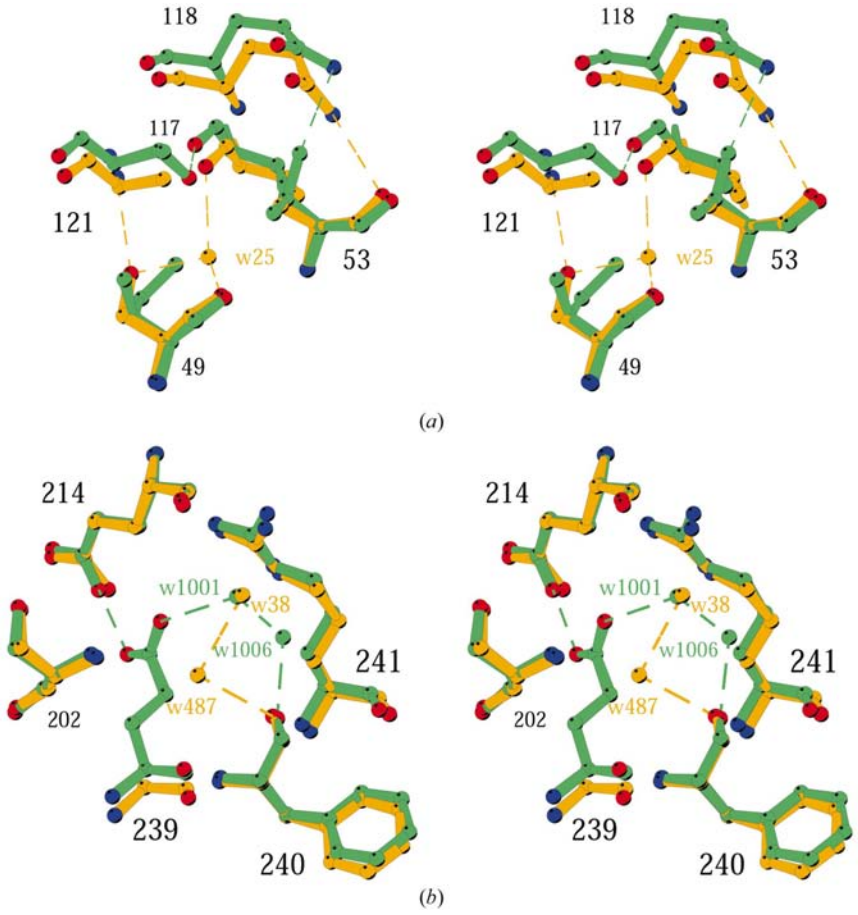

Figure 5
Superposition of TS-rCiP (yellow) and rCiPON-RT (green) (*a*) at the I49S, V53A and T121A sites and (*b*) at the E239G site. The figures are stereoviews prepared using the program *MOLSCRIPT* (Kraulis, 1991).

consisting of residues 137–150; this suggests a higher degree of ordering of the loop containing this region, which could be a consequence either of the lower temperature or of the increased thermostability of the enzyme.

3.4. The substituted sites

The structural comparison described above did not reveal any significant changes in the folding of TS-rCiP compared with the wild-type enzyme and the smaller mobility of one loop region could be an effect of the lower temperature; an examination of the substituted sites was therefore conducted, as illustrated in Fig. 3.

The I49S, V53A and T121A substitutions improved both the thermostability and the oxidative stability, independently and synergestically (Cherry *et al.*, 1999). The most significant difference between the structure of TS-rCiP and rCiPON-RT is the introduction of a water molecule (W25) in a pocket between helices *B* and *D* (see Fig. 5). This pocket is delineated by residues 49 and 53 (helix *B*) and residues 117, 118 and 121 (helix *D*). The water molecule is part of a network of hydrogen bonds which connects the two sides of the pocket. W25 donates its protons to the backbone carbonyl groups of Ser49 and Ile117 and accepts a proton from the side-chain hydroxyl group of Ser49, which also accepts a proton from the backbone amino group of Ala121. The water molecule at the position of W25 is not observed in the native structure, where the hydrophobic side chain of Ile49 points into the pocket and would make the pocket unfavourable for a water molecule. The isopropyl group of Val53 is close (3.26/3.32 Å) to the amide group of the side chain of Gln118. This interaction is probably repulsive, as in TS-rCiP an additional hydrogen bond is formed between the amide group and the backbone carbonyl group of Ala53. The hydrogen bond between the side-chain hydroxyl group of Thr121 and the backbone carbonyl group of Ile117 in the native structure is lost in TS-rCiP. The interactions described above are summarized in Table 2. The synergistic effect is partly a consequence of the rearrangment of the intrahelical and interhelical hydrogen bonds of helices *B* and *D* caused by the three substituted residues. Interhelical hydrogen bonds are formed at the expense of an intrahelical hydrogen bond.

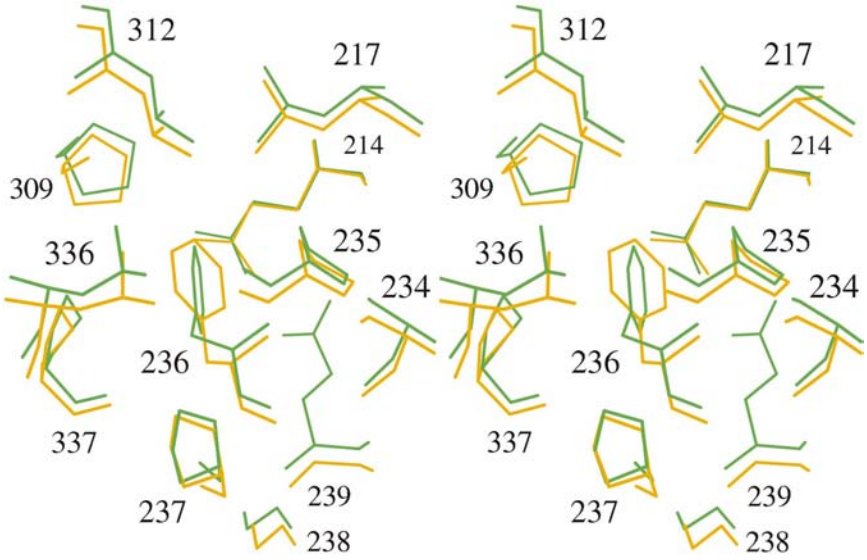

Figure 6
Superposition of TS-rCiP (yellow) and rCiPON-RT (green) at residue Phe236. The figure is a stereoview prepared using the program *MOLSCRIPT* (Kraulis, 1991).

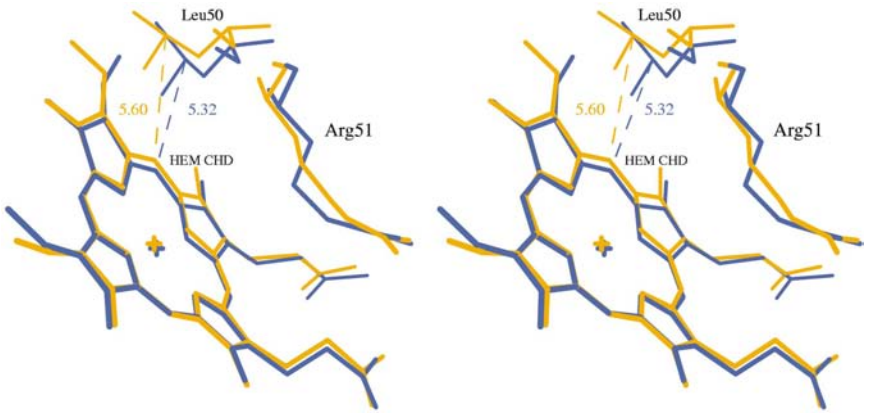

Figure 7
Superposition of the haem groups of TS-rCiP (black) and rCiPON-LT (blue). The figures are stereoviews prepared using the program *MOLSCRIPT* (Kraulis, 1991).

The E239G substitution was created to remove a potentially destabilizing interaction at high pH between two structurally adjacent glutamic acid side chains Glu239 and Glu214 (Cherry *et al.*, 1999) and led also to improved thermostability. When one of the two glutamic acids is protonated, the two carboxylic acid groups will be hydrogen bonded. At high pH, when both carboxylic groups are deprotonated, they will repel each other. The thermostability at high pH of a mutant enzyme in which only the E239G substitution had been made was improved 146 times compared with the native enzyme CiP (Cherry *et al.*, 1999). Fig. 5 illustrates the residues around the E239G site for TS-rCiP and rCiPON-RT. Changing the side chain from glutamic acid in the native structure to glycine in the mutant enzyme does not change the position of the other side chains nor the number of water molecules found in the vicinity of the altered region. Though both TS-rCiP and rCiPON-RT have two water molecules, only one occupies a common site (W38 in TS-rCiP and W1001 in rCiPON-RT), where it is hydrogen bonded to the side chain (N^{ε}) of Arg241. The other water molecule (W487 in TS-rCiP and W1006 in rCiPON-RT) is

hydrogen bonded to the backbone carbonyl group of Phe240 in both structures, although it adopts different positions in the structures. W487 is found in the region of the missing side chain of the substituted residue, whereas W1006 is located close to Arg241. Phe236 is located close to E239G; the change from a glutamic acid to a glycine at this site leads to significant changes in the position of Phe236. The aromatic ring of the phenylalanine in TS-rCiP is rotated by approximately 45° relative to its position in rCiPON-RT, as illustrated in Fig. 6. The position of the surrounding residues as well as the contacts between the phenylalanine and the nearby residues differ in the two crystal structures. An unusually short distance (3.13/3.20 Å) between Phe236 C^{β} and Pro237 C^{δ} is found in rCiPON-RT. This could arise from the fact that the position of the backbone of rCiPON-RT is restrained owing to hydrogen bonding between the glutamic acid side chains of Glu214 and Glu239. The different position of the backbone could provide space that allows the phenylalanine to adopt a more favourable conformation. The differences in interatomic distances around the E239G site are given in Table 2.

The M166F, M242I and Y272F substitutions were designed to remove oxidizable residues close to the haem group (Cherry *et al.*, 1999). Both methionine and tyrosine can be oxidized by hydrogen peroxide, whereas the residues introduced, phenylalanine and isoleucine, are not oxidized. It has been shown that these substitutions only affect the oxidative stability of the enzyme (Cherry *et al.*, 1999). Examination of the sites of the substitutions methionine to isoleucine and tyrosine to phenylalanine in TS-rCiP showed that they are very similar to the equivalent sites in rCiPON-RT, as might be expected. The third substitution of a methionine by a phenylalanine did not alter the nearby residues since there is sufficient space in the structure for the phenylalanine substitution. Since the M166F, M242I and Y272F substitutions are located around the haem group, it was examined to find out if the sustitutions had modified the haem-binding site. The rCiPON-LT model (PDB code 1lyc) was used in this comparison since it also is based on data from cryocooled crystals; it has been shown that either the use of glycerol as a cryoprotectant or the lowering of the temperature influences the environment of the haem group (Houborg *et al.*, 2003). The two structures from cryocooled crystals do not contain any solvent molecules between Fe^{III} and His55. Superimposing the two X-ray crystal structures shows that the haem groups bend in a similar way (see Fig. 7). However, the side chain of Arg51, which is located close to the haem group, adopts a slightly different conformation, as seen in Fig. 7. However, this does not change any hydrogen bonds since the guanidinium group with the three N atoms is maintained at the same position.

4. Conclusion

A structural explanation for the higher thermostability and oxidative stability of TS-rCiP containing seven substitutions in the 343 amino-acid chain compared with the native CiP has been provided. The higher thermostability and oxidative stability can be attributed partly to the rearrangement of intrahelical and interhelical hydrogen bonds which involve a water molecule introduced into TS-rCiP. Other rearrangements in the hydrogen-bond system are also seen in a single substitution which has been shown to improve thermostability. Changes of the oxidizable amino acids are not accompanied by any significantly structural changes.

We would like to thank Ulla Rosenberg and Flemming Hansen for technical support and Dr Renuka Kadirvelraj for help with the crystallization experiment. The authors are grateful to MAX-lab, Lund, Sweden for providing beam time for the project, and to DANSYNC and the EU for contribution to travel expenses under the 'Access to Research Infrastructures' program. The project was supported by the Danish National Research Foundation and a Novo Nordisk Scholarship.

References

Brünger, A. T., Adams, P. D., Clore, G. M., DeLano, W. L., Gros, P., Grosse-Kunstleve, R. W., Jiang, J.-S., Kuszewski, J., Nilges, M., Pannu, J. S., Read, R. J., Rice, L. M., Simonson, T. & Warren, G. L. (1998). *Acta Cryst.* D**54**, 905–921.

Cerenius, Y., Ståhl, K., Svensson, L. A., Ursby, T., Oskarsson, Å., Albertsson, J. & Liljas, A. (2000). *J. Synchrotron Rad.* **7**, 203–208.

Cherry, J. R., Lamsa, M. H., Schneider, P., Svendsen, A., Jones, A. & Pedersen, A. H. (1999). *Nature Biotechnol.* **17**, 379–384.

Collaborative Computational Project, Number 4 (1994). *Acta Cryst.* D**50**, 760–763.

Cudney, R., Patel, S., Weisgraber, K., Newhouse, Y. & McPherson, A. (1994). *Acta Cryst.* D**50**, 414–423.

Harris, P., Poulsen, J.-C. N., Jensen, K. F. & Larsen, S. (2002). *J. Mol. Biol.* **318**, 1019–1029.

Houborg, K., Harris, P., Petersen, J., Rowland, P., Poulsen, J.-C. N., Schneider, P., Vind, J. & Larsen, S. (2003). *Acta Cryst.* D**59**, 989–996.

Kjalke, M., Andersen, M. B., Schneider, P., Christensen, B., Schülein, M. & Welinder, K. (1992). *Biochim. Biophys. Acta*, **1120**, 248–256.

Kleywegt, G. J., Zou, J. Y.. Keldgaard, M. & Jones, J. A. (2001). *International Tables For X-ray Crystallography*, Vol. F, edited by M. G. Rossmann & E. Arnold, pp. 353–356 and 366–367. Dordrecht: Kluwer Academic Publishers.

Kraulis, P. J. (1991). *J. Appl. Cryst.* **24**, 946–950.

Kunishima, N., Fukuyama, K. & Matsubara, H., (1994). *J. Mol. Biol.* **235**, 331–334.

Navaza, J. & Saludjian, P. (1997). *Methods Enzymol.* **276**, 581–594.

Otwinowski, Z. & Minor, W. (1997). *Methods Enzymol.* **20**, 307–326.

Petersen, J. F. W., Kadziola, A. & Larsen, S. (1994). *FEBS Lett.* **339**, 291–296.

Petersen, J. F. W., Tams, J. W., Vind, J., Svensson, A., Dalbøge, H., Welinder, K. G. & Larsen, S. (1993). *J. Mol. Biol.* **232**, 989–991.

Roussel, A. & Cambillau, C. (1992). *TURBO-FRODO.* Biographics and AFMB (Architecture et Fonction des Macromolécules Biologiques), Marseille, France.

Stura, E. A., Nemerow, G. R. & Wilson, I. A. (1992). *J. Cryst. Growth*, **122**, 273–285.

Sawai-Hatanaka, H., Ashikari, T., Tanaka, Y., Nakayama, T., Minakata, H., Kunishima, N., Fukuyama, K., Yamada, H., Shibano, Y. & Amachi, T. (1995). *Biosci. Biotechnol. Biochem.* **59**, 1221–1228.

Welinder, K. G. (1992). *Curr. Opin. Struct. Biol.* **2**, 388–392.